HHS Public Access

Author manuscript

Cell Rep. Author manuscript; available in PMC 2018 January 22.

Published in final edited form as:

Cell Rep. 2017 September 05; 20(10): 2408–2423. doi:10.1016/j.celrep.2017.08.041.

Long noncoding RNA *PURPL* suppresses basal p53 levels and promotes tumorigenicity in colorectal cancer

Xiao Ling Li[1,*], **Murugan Subramanian**[1,*], **Matthew F. Jones**[1,*], **Ritu Chaudhary**[1], **Deepak K. Singh**[2], **Xinying Zong**[2], **Berkley Gryder**[3], **Sivasish Sindri**[3], **Min Mo**[4], **Aaron Schetter**[5], **Xinyu Wen**[3], **Swetha Parvathaneni**[6], **Dickran Kazandjian**[5], **Lisa M. Jenkins**[7], **Wei Tang**[8], **Fathi Elloumi**[9], **Jennifer L. Martindale**[10], **Maite Huarte**[11], **Yuelin Zhu**[12], **Ana I. Robles**[5], **Susan M. Frier**[13], **Frank Rigo**[13], **Maggie Cam**[9], **Stefan Ambs**[8], **Sudha Sharma**[6], **Curtis C. Harris**[5], **Mary Dasso**[4], **Kannanganattu V. Prasanth**[2], and **Ashish Lal**[1,#]

[1]Regulatory RNAs and Cancer Section, Genetics Branch, Center for Cancer Research (CCR), National Cancer Institute (NCI), National Institutes of Health (NIH), Bethesda, MD 20892, USA

[2]Department of Cell and Developmental Biology, University of Illinois at Urbana-Champaign, Urbana, IL 61801, USA

[3]Oncogenomics Section, Genetics Branch, CCR, NCI, NIH, Bethesda, MD 20892, USA

[4]Laboratory of Gene Regulation and Development, National Institute of Child Health and Human Development, NIH, Bethesda, MD 20892, USA

[5]Molecular Genetics and Carcinogenesis Section, Laboratory of Human Carcinogenesis, CCR, NCI, NIH, Bethesda, MD 20892, USA

[6]Department of Biochemistry and Molecular Biology, College of Medicine, Howard University, Washington, DC 20059, USA

[7]Laboratory of Cell Biology, CCR, NCI, NIH, Bethesda, MD 20892, USA

[8]Molecular Epidemiology Section, Laboratory of Human Carcinogenesis, CCR, NCI, NIH, Bethesda, MD 20892, USA

[9]Office of Science and Technology Resources, CCR, NCI, NIH, Bethesda, MD 20892, USA

[10]Laboratory of Genetics, National Institute on Aging-Intramural Research Program, NIH, Baltimore, MD 21224, USA

[#]**Corresponding author:** ashish.lal@nih.gov.
[*]These authors contributed equally to this work.
Lead contact: Ashish Lal, ashish.lal@nih.gov

ACCESSION NUMBERS

The accession number for the RNA-seq data deposited for this paper is GSE79249 and accession number for the microarray data is GSE79053.

AUTHOR CONTRIBUTIONS

Conceived and designed the experiments: Li.X., S.M., J.M.F., L.A. Performed experiments: S.D.K., Z.X., M.M., C.R., R.C., P.S., J.K., M.J., L.A. Contributed materials/tools and performed data analysis: G.B., S.S., S.A., W.X., K.D., J.L., T.W., E.F., H.M., Z.Y., C.M., A.A., H.C.C., D.A., F.S., R.F. Wrote the manuscript: Li.X., J.M.F., L. A. Edited the manuscript: Li, X, J.M.F., P.K.V., L.A.

[11]Center for Applied Medical Research, Department of Gene Therapy and Regulation of Gene Expression, University of Navarra, 31008 Pamplona, Spain

[12]Molecular Genetics Section, Genetics Branch, CCR, NCI, NIH, Bethesda, MD 28092, USA

[13]Ionis Pharmaceuticals, Carlsbad, CA 92010, USA

SUMMARY

Basal p53 levels are tightly suppressed under normal conditions. Disrupting this regulation results in elevated p53 levels to induce cell cycle arrest, apoptosis and tumor suppression. Here, we report the suppression of basal p53 levels by a nuclear, p53-regulated long noncoding RNA that we termed *PURPL* (p53 upregulated regulator of p53 levels). Targeted depletion of *PURPL* in colorectal cancer cells results in elevated basal p53 levels and induces growth defects in cell culture and in mouse xenografts. *PURPL* associates with MYBBP1A, a protein that binds to and stabilizes p53, and inhibits the formation of the p53-MYBBP1A complex. In the absence of *PURPL*, MYBBP1A interacts with and stabilizes p53. Silencing MYBBP1A significantly rescues basal p53 levels and proliferation in *PURPL*-deficient cells, suggesting that MYBBP1A mediates the effect of *PURPL* in regulating p53. These results reveal a p53-*PURPL* autoregulatory feedback loop and demonstrate a role for *PURPL* in maintaining basal p53 levels.

eTOC blurb

For a cell to divide, the tumor suppressor protein p53 must be kept at low levels. Li et al. find that a long noncoding RNA PURPL allows cancer cells to divide by keeping p53 levels low. PURPL binds to the p53-regulator MYBBP1A to suppress p53 levels and facilitate cell proliferation.

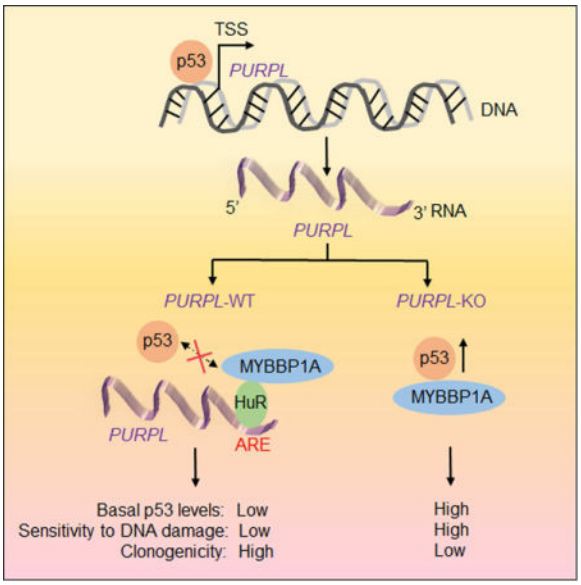

Keywords

lncRNA; lincRNA; *PURPL*; p53; HuR; MYBBP1A; *LOC643401*; *LINC01021*; *RP11-46C20.1*; CRC; CRISPR/Cas9

INTRODUCTION

Long noncoding RNAs (lncRNAs) are an emerging class of regulatory RNAs, >200 nucleotides (nt) long. The mammalian genome is transcribed into thousands of uncharacterized lncRNAs (Iyer et al., 2015, Ulitsky and Bartel, 2013) but only a few lncRNAs including *HOTAIR*, *MALAT1*, *NORAD*, *XIST* and *CCAT2* have established biological functions (Lee et al., 2016, Lee, 2012, Tripathi et al., 2013, Tripathi et al., 2010, Fatica and Bozzoni, 2014, Engreitz et al., 2013, Arun et al., 2016, Ling et al., 2013, Redis et al., 2016, Mueller et al., 2015, Dey et al., 2014, Rinn et al., 2007, Li et al., 2013, Gupta et al., 2010).

Most lncRNAs are less conserved than mRNAs and are often expressed at low levels in a cell-type or tissue-specific manner (Tsoi et al., 2015). Therefore, it is difficult to predict whether a given lncRNA is functional or reflects transcriptional noise. LncRNAs are regulated by the same transcription factors that regulate protein-coding genes, and increasing evidence suggests that the master-regulatory transcription factor p53, controls the expression of subset of lncRNAs (Grossi et al., 2016, Chaudhary and Lal, 2016, Adriaens et al., 2016, Mello et al., 2017, Chaudhary et al., 2017). Coordinated regulation of even low-abundance lncRNAs indicates that many lncRNAs have undiscovered, yet critical functions in cell biology and disease.

The tumor suppressor p53 is mutated in more than 50% of human cancers (Vogelstein et al., 2000, Vousden and Lane, 2007). In response to stress such as DNA damage, p53 directly activates the transcription of a myriad of protein-coding genes that control a wide variety of cellular processes, including cell cycle arrest, apoptosis and senescence (Bieging and Attardi, 2012, Riley et al., 2008, Beckerman and Prives, 2010). We and others have shown that p53 also directly upregulates several microRNAs including *miR-34a* and *miR-3189*, which, in turn, suppress gene expression downstream of p53 (Chang et al., 2007, Lal et al., 2011, Hermeking, 2012, Jones et al., 2015, Raver-Shapira et al., 2007). More recently, we and others have demonstrated specific functions of a number of p53-regulated lncRNAs, including *lincRNA-p21*, *PANDA*, *DINO*, *PINT*, *PR-lncRNA-1*, *LED*, *linc-475*, *NEAT1* and *PINCR* (Huarte et al., 2010, Dimitrova et al., 2014, Hung et al., 2011, Marin-Bejar et al., 2013, Sanchez et al., 2014, Leveille et al., 2015, Melo et al., 2016, Schmitt et al., 2016, Adriaens et al., 2016, Mello et al., 2017, Chaudhary et al., 2017). Although these studies illustrate the importance of lncRNAs in the p53 network as well as the functional heterogeneity of p53-regulated lncRNAs, the function of the vast majority of p53-regulated lncRNAs remains to be elucidated.

In this study, we investigated the function of a p53-regulated lncRNA that we named *PURPL* (p53 upregulated regulator of p53 levels). *PURPL* is an intergenic lncRNA that we identified by RNA-seq from multiple colorectal cancer (CRC) lines. We show that loss of *PURPL* results in elevated basal p53 levels and impaired cell growth *in vitro* and *in vivo*. *PURPL* regulates basal p53 levels by associating with MYBBP1A, a protein known to bind to and activate p53 (Ono et al., 2014, Kuroda et al., 2011, Kumazawa et al., 2015). Altogether, our study provides functional insights on *PURPL*, demonstrating a role of this lncRNA in suppressing basal p53 levels.

RESULTS

Identification and characterization of *PURPL*

To identify lncRNAs regulated by p53 in multiple CRC cell lines, we performed paired-end Ribo-zero RNA-seq from p53 wild-type (WT) and isogenic p53 knockout (KO) HCT116, RKO and SW48 cells under untreated condition or after DNA damage induced by Doxorubicin (DOXO) for 16 hr at a final concentration of 300 nM. Using a cut-off of 1.50-fold change, 511 transcripts were upregulated upon DOXO-treatment in a p53-dependent manner in all 3 CRC lines (Table S1 and Figure S1A). Although hundreds of annotated intergenic lncRNAs (lincRNAs) were induced in a p53-dependent manner in each cell line, only 33 were upregulated in all 3 lines. The overlap was more substantial between HCT116 and RKO; 230 lincRNAs were upregulated in both HCT116 and RKO. As positive controls, several well-established p53-regulated genes including *p21* (*CDKN1A*), *GDF15* and *MDM2* were upregulated in all 3 lines (Figure 1A). The 33 lincRNAs included the p53-regulated *PINCR*, *PR-lncRNA-1*, *LncRNA-4* and *LncRNA-7* (Younger et al., 2015, Sanchez et al., 2014, Chaudhary et al., 2017); other p53-regulated lncRNAs such as *NORAD, LED* and *linc-475* (Melo et al., 2016, Leveille et al., 2015, Lee et al., 2016) were upregulated in at least one of the 3 lines.

Our RNA-seq identified *RP11-46C20.1*/*LOC643401*/*LINC01021*, which we termed *PURPL*, an abundant lincRNA upregulated after DNA damage in a p53-dependent manner in all 3 lines (Figures 1A and 1B). Although RefSeq predicts a single multi-exonic transcript (*LINC01021*), according to GENCODE version 19 and ENSEMBL version 75, 6 transcripts are expressed from the *PURPL* locus (Figure S1B). In addition, we noticed a substantial signal from intron 2 (Figure 1B), also observed in a recent study from MCF7 cells (Leveille et al., 2015). RT-qPCR using exon-exon and exon-intron primers indicated that intron 2 may be retained and that exons 4 and 5 were expressed at low levels (Figure S1C), possibly due to co-transcriptional degradation of this lncRNA as recently reported (Schlackow et al., 2017).

We validated the p53-dependent upregulation of *PURPL* by RT-qPCR upon genetic loss of p53 (Figure S2A) or upon p53 knockdown (Figure S2B) in HCT116 in the presence or absence of DOXO. To determine if *PURPL* is a direct p53 target, we utilized published p53 ChIP-seq data from HCT116, MCF7 and U2OS cells (Nikulenkov et al., 2012, Sanchez et al., 2014, Menendez et al., 2013). We observed a strong p53 ChIP-seq signal (Figure S2C) located ~130 base pairs (bp) upstream of *PURPL* exon 1 and validated this result in HCT116 cells by ChIP-qPCR (Figure S2D). In contrast to these lines that express p53WT, knockdown of mutant p53 in HT29 and SW480 cells had no effect on *PURPL* levels (Figure S2E), demonstrating that *PURPL* expression is regulated by p53WT. During the course of our study, regulation of *PURPL* by p53 was also observed by others (Leveille et al., 2015, Hunten et al., 2015, Younger et al., 2015). Because the physiological function of *PURPL* was not known, we investigated a potential role of this lncRNA in the p53 network.

LncRNAs can be nuclear and/or cytoplasmic. RT-qPCR from nuclear and cytoplasmic fractions (Figure 1C) and RNA fluorescence *in situ* hybridization (RNA-FISH) (Figure S3A) suggested that a majority of *PURPL* is in the nucleus. Next, RT-qPCR from HCT116 total

RNA and *in vitro* transcribed *PURPL* RNA revealed that *PURPL* is expressed at ~6 molecules per cell in untreated condition and ~60 molecules per cell after DOXO treatment (Figure S3B). We identified a canonical polyadenylation signal at the 3′end of *PURPL* (Figure S3C) and found that *PURPL* has extremely low coding potential (Figure S3D). To determine the stability of this lncRNA, we treated HCT116 cells with Actinomycin D (Act D) for 0, 2, 4 and 8 hr and measured *PURPL* levels by RT-qPCR. Unlike the very stable *MALAT1* with a reported half-life of >9 hr (Tani et al., 2010, Tani et al., 2012), we found that the half-life of *PURPL* was ~2.5 hr (Figure S3E), suggesting that *PURPL* is an unstable lncRNA. As a positive control, more than 90% of *MYC* mRNA was lost by 2 hr of Act D treatment (Figure S3F).

Targeted depletion of *PURPL* using CRISPR/Cas9 uncovers its pro-survival function

In response to DNA damage, some p53 targets (e.g., *PUMA, DINO* and *lincRNA-p21*) are pro-apoptotic (Huarte et al., 2010, Dimitrova et al., 2014, Schmitt et al., 2016) whereas others such as *p21*, *14-3-3σ*, *PANDA* and *PINCR* are pro-survival (Bunz et al., 1998, Chan et al., 1999, Hung et al., 2011, Villunger et al., 2003, Chaudhary et al., 2017). We therefore asked whether *PURPL* is a pro-apoptotic or a pro-survival lncRNA. Because even basal *PURPL* levels are controlled by p53 and there was a single p53 ChIP-seq peak in the *PURPL* promoter (Figure S2), we decided to generate mutations in this region in HCT116 using CRISPR/Cas9. Under this p53 ChIP-seq peak, there were two p53-response elements (p53REs), of which the left p53RE was much more similar to the canonical p53RE (Figures S4A–C). When we performed CRISPR/Cas9 followed by Sanger sequencing from 34 clones, we found 2 clones in which there were mutations in the p53 ChIP-seq peak region (Figure S4D). These clones were therefore designated as *PURPL*-KO#1 and *PURPL*-KO#2. For negative controls, we selected 2 wild-type clones in which the p53REs were intact and designated these as *PURPL*-WT#1 and *PURPL*-WT#2. In both KO clones, the left p53RE was intact but there were mutations in the right p53RE. Importantly, in the 2 KO clones, both basal and induced *PURPL* levels were dramatically (>90%) reduced (Figure 2A). In addition, binding of p53 to the *PURPL* promoter was completely lost after DOXO-treatment (Figure S4E) and deleting the left or the right p53RE resulted in reduced basal and induced luciferase expression in promoter reporter assays (Figure S4F).

We next treated *PURPL*-WT and *PURPL*-KO cells with DOXO and assessed the effect on cell cycle arrest and apoptosis by performing propidium iodide (PI) staining followed by flow cytometry (FACS) analysis. Both *PURPL*-KO clones displayed significantly increased cell death (>30% cells in sub-G1) and a modest decrease in the G2/M population after DNA damage (Figure 2B). Therefore, we speculated that loss of *PURPL* might result in a defective G2/M checkpoint that would disrupt the nuclear envelope and allow the cells to undergo apoptosis in M-phase by failing to arrest in G2. However, this was not the case. After DNA damage, the nuclear membrane was intact and the cells did not enter M-phase in both *PURPL*-WT and *PURPL*-KO cells as assessed by immunostaining for the nuclear envelope marker Nucleoporin (Figure 2C). Consistent with the increased sub-G1 population, a majority of the *PURPL*-KO cells stained positive for the apoptosis marker cleaved caspase-3 (Figure 2C). Thus, in the context of DNA damage, *PURPL* functions as a pro-survival p53-regulated gene.

PURPL suppresses basal p53 levels

To begin to investigate the mechanism involved, we performed microarrays from *PURPL*-WT and *PURPL*-KO cells (Table S2). A cut-off of 1.50-fold change and $p<0.05$ was used to identify differentially expressed genes. In our microarrays, the mRNA expression of the *PURPL* neighboring genes *CDH6*, *CDH9* and *CDH10* was not altered upon loss of *PURPL*. Surprisingly, loss of basal *PURPL* resulted in upregulation of several p53 target genes including *CDKN1A*, *MDM2* and *TP53INP1*. Pathway analysis revealed over-representation of p53 signaling in the upregulated gene set (Figure S5A). and loss of *PURPL* resulted in significantly increased p53 transcriptional activity driven by a p53-responsive promoter luciferase vector containing 13 consensus p53 binding sites (el-Deiry et al., 1993) (Figure S5B). Moreover, basal *p21*, *MDM2* and *NOXA* mRNAs and basal p53 and p21 protein levels were upregulated upon loss of *PURPL* (Figures 3A, 3B and S5C) suggesting that *PURPL* suppresses basal p53 levels.

We next performed a rescue experiment by re-introducing *PURPL* (*LINC01021*) in *PURPL*-KO cells. We transfected the cells for 48 hr with a mammalian expression vector (pCB6) or pCB6 in which we cloned *PURPL* using synthetic oligonucleotides (pCB6-*PURPL*). We observed up to 8-fold overexpression of *PURPL* (Figure S5D). Comparison of p53 levels normalized to GAPDH in lanes 5 vs 7 in the immunoblot in Figure 3C and lanes 1 vs 3 in Figure S5E (quantitated in Figure S5F) showed that reintroduction of *PURPL* in *PURPL*-KO cells decreased basal p53 levels in both KO clones. However, we did not observe a reproducible effect on the DOXO-induced p53 levels; compare p53 levels in lanes 6 vs 8 in Figure 3C and 2 vs 4 in Figure S5G. Interestingly, overexpression of *PURPL* in *PURPL*-WT cells decreased basal as well as DOXO-induced p53 levels (Figure 3C; quantitated in Figure S5G). Thus, basal p53 levels are consistently reduced upon overexpression of *PURPL*.

In our microarrays, we did not observe a significant difference in *p53* mRNA levels between *PURPL*-WT and *PURPL*-KO cells (Table S2) indicating that the increased basal p53 levels is post-transcriptional. When we blocked protein synthesis using Cycloheximide (CHX), p53 was less rapidly degraded in *PURPL*-KO cells as compared to *PURPL*-WT cells (Figures 3D, 3E and S5H) indicating that the elevated basal p53 levels upon loss of *PURPL* is due to increased stability of the p53 protein.

To test if this regulation of basal p53 levels is not restricted to HCT116, we next mutated the p53RE in *PURPL* in 3 other CRC lines that included RKO, SW48 and DLD1. Unlike RKO and SW48 that are p53WT, DLD1 express mutant p53. Mutagenesis was confirmed by Sanger sequencing (Figure S6A). This mutagenesis decreased both basal and DOXO-induced *PURPL* expression in RKO and SW48 cells (Figure S6B). In DLD1, *PURPL* was not induced after DNA damage and mutation of the p53RE did not alter *PURPL* expression (Figure S6B). Moreover, basal p53 levels were elevated upon loss of *PURPL* in RKO and SW48 but not in DLD1 (Figures 3F and S6B). These data show that the observed loss of *PURPL* expression upon mutagenesis of the p53RE in its promoter, is dependent on p53WT.

We further validated these findings by knocking down this lncRNA with antisense oligos (ASOs) and performing RT-qPCR for *p21* and *PURPL* in HCT116 and SKHep1 (liver cancer, p53WT) cells. In both lines, transient knockdown of *PURPL* resulted in significant

upregulation of *p21* mRNA (Figure S7A). Moreover, knockdown of *PURPL* using ASOs resulted in increased basal p53 levels (Figures 3G, 3H and S7B) and upregulated the p53-regulated *p21* and *TP53I3* mRNAs (Figure S7D) in multiple p53WT CRC lines that included HCT116, RKO, SW48 and SK-CO-1 but not in the mutant p53-expressing DLD1 and HT29 (Figures S7C and S7D). Of note, HCT116, RKO, SW48 and DLD1 cells are microsatellite unstable (MSI) whereas SK-CO-1 and HT29 cells are microsatellite stable (MSS). Thus, *PURPL* suppresses basal p53 levels in multiple CRC lines that express p53WT regardless of MSI status.

Loss of *PURPL* results in growth defects *in vitro* and impaired tumor growth *in vivo*

Consistent with the elevated basal p53 levels in *PURPL*-KO cells, these cells showed significant growth defects *in vitro* as compared to *PURPL*-WT cells (Figure 4A). This reduced growth was also observed upon transient knockdown of *PURPL* in HCT116 with ASOs (Figure 4B) and in colony formation assays (Figure 4C). Next, to investigate the effects of *PURPL* loss in an *in vivo* setting, we subcutaneously injected NOD-SCID mice with *PURPL*-WT and *PURPL*-KO cells. Loss of *PURPL* resulted in significantly reduced rate of xenograft tumor growth over a period of 4 weeks (Figures 4D–F). The difference in tumor volume between *PURPL*-WT and *PURPL*-KO tumors was ~2.5-fold ($p<0.05$) as early as 14 days after injection and reached ~6-fold ($p<0.005$) after 30 days (Figure 4E). These results indicate that *PURPL* plays a role in regulating tumor cell growth, both *in vitro* and *in vivo*.

To determine the contribution of increased p53 levels in the observed growth defects and hypersensitivity to DNA damage, we transfected *PURPL*-KO cells with CTL siRNA or *p53* siRNAs. We confirmed efficient knockdown of *p53* by RT-qPCR (Figure S8A). When we performed PI staining and FACS analysis in *PURPL*-KO cells, we observed marked reduction in cell death after p53 knockdown and DOXO treatment (Figure S8B). In contrast, upon *p53* knockdown, *PURPL*-WT cells were more sensitive to DOXO (Figure S8C) consistent with literature (Bunz et al., 1999) where HCT116 were shown to be more sensitive to DOXO after p53 deletion. Thus, these results indicate a major role of p53 in the observed hypersensitivity of *PURPL*-KO cells to DOXO. Moreover, silencing p53 markedly rescued the proliferation defect of untreated *PURPL*-KO cells (Figure S8D) and transient co-depletion of *PURPL* and p53 in HCT116, partially restored cell proliferation in the absence of DNA damage (Figure S8E). These data indicate that elevated basal p53 levels play a role in the growth defects and hypersensitivity to DNA damage upon *PURPL* loss.

RNA pulldowns identify MYBBP1A as a *PURPL*-interacting protein

LncRNAs often mediate their effects by binding to RNA-binding proteins. To identify *PURPL*-interacting proteins, we incubated *in vitro* transcribed biotinylated *PURPL* (Bi-*PURPL*) or a control biotinylated luciferase (Bi-*Luc*) RNA with HCT116 whole cell lysates. We pulled down RNA-protein complexes using streptavidin beads and identified *PURPL*-associated proteins by mass spectrometry (Table S3). MYBBP1A, a protein known to stabilize p53, was strongly enriched (Figures 5A–C) in the *PURPL* pulldowns (Ono et al., 2014, Kuroda et al., 2011, Kumazawa et al., 2015, Akaogi et al., 2013). MYBBP1A is a predominantly nucleolar protein that associates with RNA and directly binds to p53 in the

nucleoplasm resulting in p53 activation and stabilization (Ono et al., 2014, Kuroda et al., 2011, Hochstatter et al., 2012, George et al., 2015). Given the known role of MYBBP1A in regulating p53, we selected MYBBP1A for further analysis.

To determine if MYBBP1A associates with *PURPL* in intact cells, we performed RNA-immunoprecipitation (RIP) from formaldehyde cross-linked HCT116. We observed significant enrichment (~8-fold) of *PURPL* but not the housekeeping mRNA *SDHA*, in the MYBBP1A IPs (Figure 5D). However, loss of *PURPL* did not alter MYBBP1A expression (Figure 5E), consistent with our microarray data. Given the known role of MYBBP1A in binding to and stabilizing p53 in the nucleoplasm, we hypothesized that *PURPL* associates with MYBBP1A in the nucleoplasm to prevent the MYBBP1A-p53 complex formation. If this is the case, MYBBP1A, p53 and *PURPL* should be localized in the nucleoplasm. MYBBP1A is a predominantly nucleolar protein but after its synthesis in the cytoplasm, it will pass through the nucleoplasm, to enter the nucleolus. p53 is also known to be present in the nucleoplasm.

To determine if *PURPL* is in the nucleoplasm, we performed subcellular fractionation in which we isolated nucleolar and nucleoplasmic fractions from HCT116 cells according to the well-established protocol from the Lamond lab (see experimental procedures). In the nucleus, majority of *PURPL* and the lncRNA *MALAT1* were nucleoplasmic (Figure 5F); the control pre-rRNA, was mostly nucleolar. The fractionation was further confirmed by immunoblotting for Histone H3 (NPL (nucleoplasmic) marker), Nucleolin (NCL (nucleolar) marker) and tubulin (CYT (cytoplasmic) marker) (Figure 5G). Next, in co-IPs from nucleoplasmic extracts, p53 was enriched in the MYBBP1A IP in *PURPL*-KO cells but not in *PURPL*-WT cells (Figure 5H). Importantly, re-introduction of *PURPL* in *PURPL*-KO cells inhibited the p53-MYBBP1A interaction (Figure S19A) and partially rescued hypersensitivity to DNA damage (Figure S9B). These data indicate that *PURPL* inhibits the formation of a MYBBP1A-p53 complex in the nucleoplasm.

HuR directly binds to *PURPL* and acts as an adaptor to recruit MYBBP1A to *PURPL*

MYBBP1A does not possess canonical RNA-binding domains but has been shown to associate with RNA via yet, unidentified RNA-binding proteins (Kuroda et al., 2011). In a recent study, *in vivo* UV-crosslinking and RNA-IP (RIP) was utilized to show direct binding of p53 to *DINO*, a p53-regulated lncRNA (Schmitt et al., 2016). To test if *PURPL* directly binds to MYBBP1A, we used this approach. We did not observe enrichment of *PURPL* in the MYBBP1A RIPs (Figure 6A). This result together with the observed association of *PURPL* with MYBBP1A from formaldehyde crosslinked cells (Figure 5D), a reagent that can crosslink proteins that indirectly associate with the RNA, indicates that MYBBP1A associates with *PURPL* but does not directly bind to this lncRNA.

We therefore hypothesized that the MYBBP1A-*PURPL* complex is formed through an adaptor protein that directly binds to this lncRNA. From our RNA pulldowns and mass spectrometry, we selected RNA-binding protein HuR as a potential adaptor protein due to the following reasons. First, HuR was strongly enriched in the *PURPL* pulldowns (Figure 6B). Second, we and others have previously shown that HuR plays a role in the p53 pathway (Lopez de Silanes et al., 2004, Lal et al., 2004, Lal et al., 2005, Mazan-Mamczarz et al.,

2003, Galban et al., 2003). Finally, HuR binds to AU-rich elements (AREs) in RNA (Lopez de Silanes et al., 2004, Lal et al., 2004) and we found a single consensus (Lebedeva et al., 2011) high affinity HuR binding motif (ARE core) at the 3′end of *PURPL* (Figure 6C).

When we performed *in vitro* RNA pulldowns. we found that Bi-*PURPL* but not Bi-*Luc* associates with HuR (Figure 6D); as a negative control, GAPDH was detected only in input (Figure 6D). Moreover, RNA pulldowns using purified recombinant GST-HuR, showed that GST-HuR directly binds to Bi-*PURPL* (Figure 6E). In RT-qPCR following HuR-RIP from UV-crosslinked HCT116 cells, ~12-fold enrichment of *PURPL* was observed in HuR RIPs indicating direct interaction of *PURPL* and HuR in intact cells (Figure 6F). To determine if HuR interacts with the ARE in *PURPL*, we performed HuR-RIP assays from UV-crosslinked HCT116 cells after sonicating the lysate before the RIP assay, to fragment the RNAs, a strategy used in the *DINO* paper (Schmitt et al., 2016). RT-qPCR with primers that span the *PURPL*-ARE or an adjacent Non-ARE region, showed that the *PURPL*-ARE was specifically enriched in the HuR IPs (Figure 6G). These data suggest that HuR directly binds to the ARE at the 3′end of *PURPL* RNA.

If HuR is the adaptor responsible for recruiting MYBBP1A to the *PURPL* RNA, HuR should interact with MYBBP1A, and silencing HuR should abrogate the *PURPL*-MYBBP1A interaction. Indeed, we found enrichment of HuR in the MYBBP1A IP (Figure 6H); the HuR-MYBBP1A complex was resistant to RNase, suggesting that HuR and MYBBP1A form a protein-protein complex (Figure 6I). Upon silencing HuR (Figure 6J) followed by MYBBP1A RIP and RT-qPCR from formaldehyde crosslinked cells, the *PURPL*-MYBBP1A interaction was lost (Figure 6K), although we pulled down comparable levels of MYBBP1A (Figure 6L). These data indicate that MYBBP1A associates with *PURPL* RNA via the adaptor protein HuR.

Silencing MYBBP1A partially rescues basal p53 levels and proliferation of *PURPL*-KO cells

We next silenced MYBBP1A in *PURPL*-WT and *PURPL*-KO cells and assessed the effect on p53 protein levels and cell proliferation. Silencing MYBBP1A partially reduced basal p53 protein levels (Figures 7A, S10A and S10B) and *p21* mRNA levels (Figure 7B) and increased proliferation only in *PURPL*-KO cells (Figure 7C), suggesting that MYBBP1A mediates the effects of *PURPL*, at least in part, by regulating basal p53 levels and cell proliferation.

To determine if our findings from cell lines are relevant to CRC, we first analyzed *PURPL* and *MYBBP1A* mRNA levels in a CRC cohort (UMMC cohort) where we have performed lncRNA arrays from 79 CRC patient samples and matched normal (Schetter et al., in preparation). Both *PURPL* RNA and *MYBBP1A* mRNA were significantly up-regulated (*PURPL:* 2.35-fold, $p<0.0001$; *MYBBP1A* mRNA: 1.44-fold $p<0.0001$) in the tumors when compared to normal tissue (Figure 7D). To determine if *PURPL* and *MYBBP1A* expression correlate with p53 mutation status, we compared *PURPL* levels between p53WT and mutant p53 tumors. Of the 79 tumor samples, 42 were p53WT and 37 had missense or nonsense *TP53* mutations. As compared to p53WT tumors, *PURPL* was significantly down-regulated (2.39-fold, $p=0.0068$) in mutant p53 tumors (Figure 7E). In addition, *PURPL* was more significantly upregulated in p53WT CRC tumors vs matched normal ($p<0.0001$) as

compared to Mutant p53 CRC tumors vs matched normal (p=0.036) (Figures S10A and S10B).

However, *MYBBP1A* mRNA levels were not significantly different between p53WT and p53 mutant tumors (Figure 7E). The higher *PURPL* levels and the unchanged *MYBBP1A* mRNA levels between p53WT tumors as compared to p53 mutant tumors is consistent with our RNA-seq data and other reports (Hunten et al., 2015, Leveille et al., 2015) where *PURPL* was identified as a p53-regulated lncRNA, whereas *MYBBP1A* is not a p53 target gene. Interestingly, when we looked at the correlation between *PURPL* and *MYBBP1A* mRNA levels in this CRC cohort, we observed significant positive correlation (correlation coefficient r=0.51, p=0.0005) between *MYBBP1A* mRNA and *PURPL* levels in p53WT tumors (Figure 7F) but not in the p53 mutant tumors (Figure S10C), which may be consistent with our data from cell lines indicating that both *PURPL* and MYBBP1A are involved in keeping basal p53 levels low. Collectively, our results identify an auto-regulatory feedback loop between p53 and *PURPL* that is mediated in part by recruitment of MYBBP1A to *PURPL* by the RNA-binding protein HuR.

DISCUSSION

In this study, we functionally characterized *PURPL*, a lncRNA directly regulated by p53 under basal conditions and after DNA damage. *PURPL* suppresses basal p53 levels, suggesting an auto-regulatory feedback loop.

It is becoming increasingly clear that even in actively dividing cells with minimal p53 activity, p53 directly activates the basal expression of many genes including *CDKN1A*, *GDF15* and *DDB2* (Allen et al., 2014, Espinosa et al., 2003, Tang et al., 1998). Using Global Run-on sequencing, it was proposed that many p53 targets are ‘primed’ before p53 activation to allow rapid upregulation of these genes upon p53 activation (Allen et al., 2014). Consistent with these findings, although *PURPL* is upregulated by p53 after DNA damage, its basal expression is also controlled by p53 in multiple CRC lines and in CRC tumors. Although p53 is inactivated in a majority of cancers, many tumors have intact p53 signaling, and therapeutic activation of p53 signaling through MDM2 inhibition is being investigated in clinical trials (Khoo et al., 2014). The significance of basal p53 signaling in cancer therapeutics was demonstrated in a recent study on a large panel of cell lines and patient-derived tumor xenografts (Espinosa and Sullivan, 2015, Jeay et al., 2015). The authors found that cell lines sensitive to p53-activating drugs had partially active p53 signaling even in the absence of the drug. *PURPL* may be a promising candidate for future translational research since *PURPL* loss can elevate basal p53 to impair proliferation, induce cell death in response to genotoxic agents and inhibit tumorigenicity *in vivo*. However, it will be important to determine the function of *PURPL* in normal cells.

Our study contributes to the emerging concept that lncRNAs acts as guides, decoys or scaffolds to control cellular processes. This has been shown previously in the context of p53: *lincRNA-p21* functions as a transcriptional repressor in the p53 pathway and modulates the localization of hnRNPK (Huarte et al., 2010, Dimitrova et al., 2014). *PANDA*, another p53-regulated lncRNA transcribed from a locus upstream of *p21*, interacts with the transcription

factor NF-YA to regulate the expression of pro-apoptotic genes during DNA damage (Hung et al., 2011). In addition, *NORAD* is indirectly regulated by p53 and plays a critical role in maintaining genomic stability by functioning as a decoy and regulates the association of the RNA-binding protein PUMILIO to its target mRNAs (Lee et al., 2016). A recent study showed that the p53-regulated lncRNA *DINO* directly binds to the C-terminal domain of p53 and regulates p53 levels in response to DNA damage (Schmitt et al., 2016).

PURPL suppresses basal p53 levels, in part, by preventing the p53-MYBBP1A complex formation in the nucleoplasm. To further support this regulation, it would be important to estimate, the number of molecules of *PURPL*, p53 and MYBBP1A in the nucleoplasm, to determine if they are present in stoichiometric amounts. Further experiments are needed to determine if this mechanism, the p53-dependence of *PURPL* expression and the p53-dependence of the chemosensitizing effects of *PURPL* inactivation are restricted to tumor cells that express p53WT or could also be observed in normal cells and mutant p53 cells. The role of *PURPL* in CRC and other cancers will require further analysis in multiple cohorts to determine if *PURPL* expression is associated with clinical outcome.

Future investigations on identification of other effectors of *PURPL*, determining if HuR and MYBBP1A interact directly or via other proteins, additional molecular mechanism(s) by which this lncRNA regulates p53, identifying and determining the role of other *PURPL* targets in mediating the effects of this lncRNA, will be necessary to fully understand how *PURPL* controls basal p53 levels and in determining its role in tumor initiation and progression. Finally, it will be interesting to see if depletion/deletion of p53 in *PURPL*-KO cells influences the tumorigenicity of these cells in mice.

EXPERIMENTAL PROCEDURES

Ribo-zero paired-end RNA-Seq and bioinformatic analysis

The isogenic p53WT and p53KO HCT116, RKO and SW48 cells were untreated or treated with DOXO (300 nM) for 16 hr and total RNA was isolated using RNeasy kit (Qiagen). Total RNA was fragmented and the cleaved RNA fragments were copied into first strand cDNA using reverse transcriptase and random primers, followed by second strand cDNA synthesis using DNA polymerase I and RNase H. The resulting double-strand cDNA was used as the input to a standard Illumina library prep with end-repair, adapter ligation and PCR amplification being performed to generate a library that would go on to the HiSeq2000 instrument for sequencing. The HiSeq Real Time Analysis software (RTA 1.18.64) was used for processing image files, the Illumina BCL2fastq1.8.4 was used for demultiplex and converting binary base calls and qualities to FASTQ format. The sequencing reads were trimmed adapters and low quality bases using Trimmomatic (version 0.3), the trimmed reads were aligned to human hg19 reference genome (GRCh37/UCSC hg19) and Ensembl annotation version 70 using TopHat_v2.0.8 software. Hundred bases long paired-end reads were assessed for quality using PICARD and FastQC. The generated FASTQ files were mapped using TopHat2 alignment algorithm. Differential gene expression analysis was performed using Cufflinks and Cuffdiff. Average read length was 110 nucleotides and we had ~ 150 million mapped reads per sample. For a non-zero-fold change, we added 0.01 to the FPKM of each gene.

UMMC (University of Maryland Medical Center) cohort analysis

Pairs of primary colon tumor and adjacent non-tumorous tissues came from 83 patients recruited from the University of Maryland Medical Center or Baltimore Veterans Affairs Medical Center between 1993 and 2002. Cases with familial adenomatous polyposis or human nonpolyposis colorectal cancer were excluded from this study. Tissues were flash frozen after surgery. Detailed backgrounds for each tissue donor, including age, sex, clinical staging, tumor location, and receipt of adjuvant chemotherapy have been collected. Tumor histopathology was classified according to the World Health Organization Classification of Tumor system. RNA from frozen tissue samples was extracted using standard TRIZOL (Invitrogen, Carlsbad, California) methods. *TP53* mutation status was determined by sequencing all *TP53* exons. The microarrays were SurePrint G3 Human Gene Expression 8×60K Microarray Kit and performed following the manufacturer's instructions.

Targeted deletion using CRISPR/Cas9

An All-in-one construct expressing GFP, the human codon-optimized Streptococcus pyogenes Cas9 Nickase mutant and the 2 gRNAs targeting the p53RE in the *PURPL* promoter was designed and purchased from DNA2.0 (https://www.dna20.com/). To select *PURPL*-WT and *PURPL*-KO clones, HCT116 were transfected with 5 μg of the all-in-one construct and after 48 hr, GFP positive cells were FACS sorted. The GFP positive cells were seeded at 1 cell per well of 96-well plates in 100 μl of DMEM. After 3 weeks, clones were harvested and split into two 24-well plates. Total RNA was isolated from a 24-well plate and *PURPL* expression was measured by RT-qPCR normalized to *GAPDH*. Genomic DNA from individual clones with dramatically reduced *PURPL* expression was extracted, and the DNA flanking the p53RE of *PURPL* was PCR amplified and subjected to Sanger sequencing.

Xenograft assays

Animal protocols were approved by the National Cancer Institute Animal Care and Use Committee following AALAAC guidelines and policies. HCT116 *PURPL*-WT and *PURPL*-KO cells were trypsinized and washed with PBS. Live cells were counted with trypan blue exclusion and equal numbers of live cells were injected for each clone. Cells (1×10^6) were mixed with 30% matrigel in PBS on ice and the mixture was injected into the flanks of 6–8-week-old female athymic nude mice (Animal Production Program, Frederick, MD, USA) (each group N=10). Tumor volume was measured twice a week after 1 week of injection.

Supplementary Material

Refer to Web version on PubMed Central for supplementary material.

Acknowledgments

We thank Bert Vogelstein for the isogenic cell lines, Myriam Gorospe for the GST and GST-HuR proteins and Tom Misteli, Susan Gottesman, Shiv Grewal and Glenn Merlino for their comments on this manuscript. This research was supported by the Intramural Research Program (A.L., S. A., C. C. H) of the National Cancer Institute (NCI), Center for Cancer Research (CCR), NIH and the NIGMS/NIH grant 5SC1GM093999-06 (S.S). K.V.P lab is supported by grants from NIH [GM088252] and American Cancer Society [RSG-11-174-01-RMC].

References

ADRIAENS C, STANDAERT L, BARRA J, LATIL M, VERFAILLIE A, KALEV P, BOECKX B, WIJNHOVEN PW, RADAELLI E, VERMI W, LEUCCI E, LAPOUGE G, BECK B, VAN DEN OORD J, NAKAGAWA S, HIROSE T, SABLINA AA, LAMBRECHTS D, AERTS S, BLANPAIN C, MARINE JC. p53 induces formation of NEAT1 lncRNA-containing paraspeckles that modulate replication stress response and chemosensitivity. Nat Med. 2016; 22:861–8. [PubMed: 27376578]

AKAOGI K, ONO W, HAYASHI Y, KISHIMOTO H, YANAGISAWA J. MYBBP1A suppresses breast cancer tumorigenesis by enhancing the p53 dependent anoikis. BMC Cancer. 2013; 13:65. [PubMed: 23388179]

ALLEN MA, ANDRYSIK Z, DENGLER VL, MELLERT HS, GUARNIERI A, FREEMAN JA, SULLIVAN KD, GALBRAITH MD, LUO X, KRAUS WL, DOWELL RD, ESPINOSA JM. Global analysis of p53-regulated transcription identifies its direct targets and unexpected regulatory mechanisms. Elife. 2014; 3:e02200. [PubMed: 24867637]

ARUN G, DIERMEIER S, AKERMAN M, CHANG KC, WILKINSON JE, HEARN S, KIM Y, MACLEOD AR, KRAINER AR, NORTON L, BROGI E, EGEBLAD M, SPECTOR DL. Differentiation of mammary tumors and reduction in metastasis upon Malat1 lncRNA loss. Genes Dev. 2016; 30:34–51. [PubMed: 26701265]

BECKERMAN R, PRIVES C. Transcriptional regulation by p53. Cold Spring Harb Perspect Biol. 2010; 2:a000935. [PubMed: 20679336]

BIEGING KT, ATTARDI LD. Deconstructing p53 transcriptional networks in tumor suppression. Trends Cell Biol. 2012; 22:97–106. [PubMed: 22154076]

BUNZ F, DUTRIAUX A, LENGAUER C, WALDMAN T, ZHOU S, BROWN JP, SEDIVY JM, KINZLER KW, VOGELSTEIN B. Requirement for p53 and p21 to sustain G2 arrest after DNA damage. Science. 1998; 282:1497–501. [PubMed: 9822382]

BUNZ F, HWANG PM, TORRANCE C, WALDMAN T, ZHANG Y, DILLEHAY L, WILLIAMS J, LENGAUER C, KINZLER KW, VOGELSTEIN B. Disruption of p53 in human cancer cells alters the responses to therapeutic agents. J Clin Invest. 1999; 104:263–9. [PubMed: 10430607]

CHAN TA, HERMEKING H, LENGAUER C, KINZLER KW, VOGELSTEIN B. 14-3-3Sigma is required to prevent mitotic catastrophe after DNA damage. Nature. 1999; 401:616–20. [PubMed: 10524633]

CHANG TC, WENTZEL EA, KENT OA, RAMACHANDRAN K, MULLENDORE M, LEE KH, FELDMANN G, YAMAKUCHI M, FERLITO M, LOWENSTEIN CJ, ARKING DE, BEER MA, MAITRA A, MENDELL JT. Transactivation of miR-34a by p53 broadly influences gene expression and promotes apoptosis. Mol Cell. 2007; 26:745–52. [PubMed: 17540599]

CHAUDHARY R, GRYDER B, WOODS WS, SUBRAMANIAN M, JONES MF, LI XL, JENKINS LM, SHABALINA SA, MO M, DASSO M, YANG Y, WAKEFIELD LM, ZHU Y, FRIER SM, MORIARITY BS, PRASANTH KV, PEREZ-PINERA P, LAL A. Prosurvival long noncoding RNA PINCR regulates a subset of p53 targets in human colorectal cancer cells by binding to Matrin 3. Elife. 2017:6.

CHAUDHARY R, LAL A. Long noncoding RNAs in the p53 network. Wiley Interdiscip Rev RNA. 2016

DEY BK, PFEIFER K, DUTTA A. The H19 long noncoding RNA gives rise to microRNAs miR-675-3p and miR-675-5p to promote skeletal muscle differentiation and regeneration. Genes Dev. 2014; 28:491–501. [PubMed: 24532688]

DIMITROVA N, ZAMUDIO JR, JONG RM, SOUKUP D, RESNICK R, SARMA K, WARD AJ, RAJ A, LEE JT, SHARP PA, JACKS T. LincRNA-p21 activates p21 in cis to promote Polycomb target gene expression and to enforce the G1/S checkpoint. Mol Cell. 2014; 54:777–90. [PubMed: 24857549]

EL-DEIRY WS, TOKINO T, VELCULESCU VE, LEVY DB, PARSONS R, TRENT JM, LIN D, MERCER WE, KINZLER KW, VOGELSTEIN B. WAF1, a potential mediator of p53 tumor suppression. Cell. 1993; 75:817–25. [PubMed: 8242752]

ENGREITZ JM, PANDYA-JONES A, MCDONEL P, SHISHKIN A, SIROKMAN K, SURKA C, KADRI S, XING J, GOREN A, LANDER ES, PLATH K, GUTTMAN M. The Xist lncRNA

exploits three-dimensional genome architecture to spread across the X chromosome. Science. 2013; 341:1237973. [PubMed: 23828888]

ESPINOSA JM, SULLIVAN KD. A signature for success. Elife. 2015:4.

ESPINOSA JM, VERDUN RE, EMERSON BM. p53 functions through stress- and promoter-specific recruitment of transcription initiation components before and after DNA damage. Mol Cell. 2003; 12:1015–27. [PubMed: 14580351]

FATICA A, BOZZONI I. Long non-coding RNAs: new players in cell differentiation and development. Nat Rev Genet. 2014; 15:7–21. [PubMed: 24296535]

GALBAN S, MARTINDALE JL, MAZAN-MAMCZARZ K, LOPEZ DE SILANES I, FAN J, WANG W, DECKER J, GOROSPE M. Influence of the RNA-binding protein HuR in pVHL-regulated p53 expression in renal carcinoma cells. Mol Cell Biol. 2003; 23:7083–95. [PubMed: 14517280]

GEORGE B, HORN D, BAYO P, ZAOUI K, FLECHTENMACHER C, GRABE N, PLINKERT P, KRIZHANOVSKY V, HESS J. Regulation and function of Myb-binding protein 1A (MYBBP1A) in cellular senescence and pathogenesis of head and neck cancer. Cancer Lett. 2015; 358:191–9. [PubMed: 25543088]

GROSSI E, SANCHEZ Y, HUARTE M. Expanding the p53 regulatory network: LncRNAs take up the challenge. Biochim Biophys Acta. 2016; 1859:200–8. [PubMed: 26196323]

GUPTA RA, SHAH N, WANG KC, KIM J, HORLINGS HM, WONG DJ, TSAI MC, HUNG T, ARGANI P, RINN JL, WANG Y, BRZOSKA P, KONG B, LI R, WEST RB, VAN DE VIJVER MJ, SUKUMAR S, CHANG HY. Long non-coding RNA HOTAIR reprograms chromatin state to promote cancer metastasis. Nature. 2010; 464:1071–6. [PubMed: 20393566]

HERMEKING H. MicroRNAs in the p53 network: micromanagement of tumour suppression. Nat Rev Cancer. 2012

HOCHSTATTER J, HOLZEL M, ROHRMOSER M, SCHERMELLEH L, LEONHARDT H, KEOUGH R, GONDA TJ, IMHOF A, EICK D, LANGST G, NEMETH A. Myb-binding protein 1a (Mybbp1a) regulates levels and processing of pre-ribosomal RNA. J Biol Chem. 2012; 287:24365–77. [PubMed: 22645127]

HUARTE M, GUTTMAN M, FELDSER D, GARBER M, KOZIOL MJ, KENZELMANN-BROZ D, KHALIL AM, ZUK O, AMIT I, RABANI M, ATTARDI LD, REGEV A, LANDER ES, JACKS T, RINN JL. A large intergenic noncoding RNA induced by p53 mediates global gene repression in the p53 response. Cell. 2010; 142:409–19. [PubMed: 20673990]

HUNG T, WANG Y, LIN MF, KOEGEL AK, KOTAKE Y, GRANT GD, HORLINGS HM, SHAH N, UMBRICHT C, WANG P, WANG Y, KONG B, LANGEROD A, BORRESEN-DALE AL, KIM SK, VAN DE VIJVER M, SUKUMAR S, WHITFIELD ML, KELLIS M, XIONG Y, WONG DJ, CHANG HY. Extensive and coordinated transcription of noncoding RNAs within cell-cycle promoters. Nat Genet. 2011; 43:621–9. [PubMed: 21642992]

HUNTEN S, KALLER M, DREPPER F, OELJEKLAUS S, BONFERT T, ERHARD F, DUECK A, EICHNER N, FRIEDEL CC, MEISTER G, ZIMMER R, WARSCHEID B, HERMEKING H. p53-Regulated Networks of Protein, mRNA, miRNA, and lncRNA Expression Revealed by Integrated Pulsed Stable Isotope Labeling With Amino Acids in Cell Culture (pSILAC) and Next Generation Sequencing (NGS) Analyses. Mol Cell Proteomics. 2015; 14:2609–29. [PubMed: 26183718]

IYER MK, NIKNAFS YS, MALIK R, SINGHAL U, SAHU A, HOSONO Y, BARRETTE TR, PRENSNER JR, EVANS JR, ZHAO S, POLIAKOV A, CAO X, DHANASEKARAN SM, WU YM, ROBINSON DR, BEER DG, FENG FY, IYER HK, CHINNAIYAN AM. The landscape of long noncoding RNAs in the human transcriptome. Nat Genet. 2015; 47:199–208. [PubMed: 25599403]

JEAY S, GAULIS S, FERRETTI S, BITTER H, ITO M, VALAT T, MURAKAMI M, RUETZ S, GUTHY DA, RYNN C, JENSEN MR, WIESMANN M, KALLEN J, FURET P, GESSIER F, HOLZER P, MASUYA K, WURTHNER J, HALILOVIC E, HOFMANN F, SELLERS WR, GRAUS PORTA D. A distinct p53 target gene set predicts for response to the selective p53-HDM2 inhibitor NVP-CGM097. Elife. 2015:4.

JONES MF, LI XL, SUBRAMANIAN M, SHABALINA SA, HARA T, ZHU Y, HUANG J, YANG Y, WAKEFIELD LM, PRASANTH KV, LAL A. Growth differentiation factor-15 encodes a novel

microRNA 3189 that functions as a potent regulator of cell death. Cell Death Differ. 2015; 22:1641–53. [PubMed: 25698447]

KHOO KH, VERMA CS, LANE DP. Drugging the p53 pathway: understanding the route to clinical efficacy. Nat Rev Drug Discov. 2014; 13:217–36. [PubMed: 24577402]

KUMAZAWA T, NISHIMURA K, KATAGIRI N, HASHIMOTO S, HAYASHI Y, KIMURA K. Gradual reduction in rRNA transcription triggers p53 acetylation and apoptosis via MYBBP1A. Sci Rep. 2015; 5:10854. [PubMed: 26044764]

KURODA T, MURAYAMA A, KATAGIRI N, OHTA YM, FUJITA E, MASUMOTO H, EMA M, TAKAHASHI S, KIMURA K, YANAGISAWA J. RNA content in the nucleolus alters p53 acetylation via MYBBP1A. EMBO J. 2011; 30:1054–66. [PubMed: 21297583]

LAL A, KAWAI T, YANG X, MAZAN-MAMCZARZ K, GOROSPE M. Antiapoptotic function of RNA-binding protein HuR effected through prothymosin alpha. EMBO J. 2005; 24:1852–62. [PubMed: 15861128]

LAL A, MAZAN-MAMCZARZ K, KAWAI T, YANG X, MARTINDALE JL, GOROSPE M. Concurrent versus individual binding of HuR and AUF1 to common labile target mRNAs. EMBO J. 2004; 23:3092–102. [PubMed: 15257295]

LAL A, THOMAS MP, ALTSCHULER G, NAVARRO F, O'DAY E, LI XL, CONCEPCION C, HAN YC, THIERY J, RAJANI DK, DEUTSCH A, HOFMANN O, VENTURA A, HIDE W, LIEBERMAN J. Capture of microRNA-bound mRNAs identifies the tumor suppressor miR-34a as a regulator of growth factor signaling. PLoS Genet. 2011; 7:e1002363. [PubMed: 22102825]

LEBEDEVA S, JENS M, THEIL K, SCHWANHAUSSER B, SELBACH M, LANDTHALER M, RAJEWSKY N. Transcriptome-wide analysis of regulatory interactions of the RNA-binding protein HuR. Mol Cell. 2011; 43:340–52. [PubMed: 21723171]

LEE JT. Epigenetic regulation by long noncoding RNAs. Science. 2012; 338:1435–9. [PubMed: 23239728]

LEE S, KOPP F, CHANG TC, SATALURI A, CHEN B, SIVAKUMAR S, YU H, XIE Y, MENDELL JT. Noncoding RNA NORAD Regulates Genomic Stability by Sequestering PUMILIO Proteins. Cell. 2016; 164:69–80. [PubMed: 26724866]

LEVEILLE N, MELO CA, ROOIJERS K, DIAZ-LAGARES A, MELO SA, KORKMAZ G, LOPES R, AKBARI MOQADAM F, MAIA AR, WIJCHERS PJ, GEEVEN G, DEN BOER ML, KALLURI R, DE LAAT W, ESTELLER M, AGAMI R. Genome-wide profiling of p53-regulated enhancer RNAs uncovers a subset of enhancers controlled by a lncRNA. Nat Commun. 2015; 6:6520. [PubMed: 25813522]

LI L, LIU B, WAPINSKI OL, TSAI MC, QU K, ZHANG J, CARLSON JC, LIN M, FANG F, GUPTA RA, HELMS JA, CHANG HY. Targeted disruption of Hotair leads to homeotic transformation and gene derepression. Cell Rep. 2013; 5:3–12. [PubMed: 24075995]

LING H, SPIZZO R, ATLASI Y, NICOLOSO M, SHIMIZU M, REDIS RS, NISHIDA N, GAFA R, SONG J, GUO Z, IVAN C, BARBAROTTO E, DE VRIES I, ZHANG X, FERRACIN M, CHURCHMAN M, VAN GALEN JF, BEVERLOO BH, SHARIATI M, HADERK F, ESTECIO MR, GARCIA-MANERO G, PATIJN GA, GOTLEY DC, BHARDWAJ V, SHUREIQI I, SEN S, MULTANI AS, WELSH J, YAMAMOTO K, TANIGUCHI I, SONG MA, GALLINGER S, CASEY G, THIBODEAU SN, LE MARCHAND L, TIIRIKAINEN M, MANI SA, ZHANG W, DAVULURI RV, MIMORI K, MORI M, SIEUWERTS AM, MARTENS JW, TOMLINSON I, NEGRINI M, BERINDAN-NEAGOE I, FOEKENS JA, HAMILTON SR, LANZA G, KOPETZ S, FODDE R, CALIN GA. CCAT2, a novel noncoding RNA mapping to 8q24, underlies metastatic progression and chromosomal instability in colon cancer. Genome Res. 2013; 23:1446–61. [PubMed: 23796952]

LOPEZ DE SILANES I, ZHAN M, LAL A, YANG X, GOROSPE M. Identification of a target RNA motif for RNA-binding protein HuR. Proc Natl Acad Sci U S A. 2004; 101:2987–92. [PubMed: 14981256]

MARIN-BEJAR O, MARCHESE FP, ATHIE A, SANCHEZ Y, GONZALEZ J, SEGURA V, HUANG L, MORENO I, NAVARRO A, MONZO M, GARCIA-FONCILLAS J, RINN JL, GUO S, HUARTE M. Pint lincRNA connects the p53 pathway with epigenetic silencing by the Polycomb repressive complex 2. Genome Biol. 2013; 14:R104. [PubMed: 24070194]

MAZAN-MAMCZARZ K, GALBAN S, LOPEZ DE SILANES I, MARTINDALE JL, ATASOY U, KEENE JD, GOROSPE M. RNA-binding protein HuR enhances p53 translation in response to ultraviolet light irradiation. Proc Natl Acad Sci U S A. 2003; 100:8354–9. [PubMed: 12821781]

MELLO SS, SINOW C, RAJ N, MAZUR PK, BIEGING-ROLETT K, BROZ DK, IMAM JFC, VOGEL H, WOOD LD, SAGE J, HIROSE T, NAKAGAWA S, RINN J, ATTARDI LD. Neat1 is a p53-inducible lincRNA essential for transformation suppression. Genes Dev. 2017; 31:1095–1108. [PubMed: 28698299]

MELO CA, LEVEILLE N, ROOIJERS K, WIJCHERS PJ, GEEVEN G, TAL A, MELO SA, DE LAAT W, AGAMI R. A p53-bound enhancer region controls a long intergenic noncoding RNA required for p53 stress response. Oncogene. 2016

MENENDEZ D, NGUYEN TA, FREUDENBERG JM, MATHEW VJ, ANDERSON CW, JOTHI R, RESNICK MA. Diverse stresses dramatically alter genome-wide p53 binding and transactivation landscape in human cancer cells. Nucleic Acids Res. 2013; 41:7286–301. [PubMed: 23775793]

MUELLER AC, CICHEWICZ MA, DEY BK, LAYER R, REON BJ, GAGAN JR, DUTTA A. MUNC, a long noncoding RNA that facilitates the function of MyoD in skeletal myogenesis. Mol Cell Biol. 2015; 35:498–513. [PubMed: 25403490]

NIKULENKOV F, SPINNLER C, LI H, TONELLI C, SHI Y, TURUNEN M, KIVIOJA T, IGNATIEV I, KEL A, TAIPALE J, SELIVANOVA G. Insights into p53 transcriptional function via genome-wide chromatin occupancy and gene expression analysis. Cell Death Differ. 2012; 19:1992–2002. [PubMed: 22790872]

ONO W, HAYASHI Y, YOKOYAMA W, KURODA T, KISHIMOTO H, ITO I, KIMURA K, AKAOGI K, WAKU T, YANAGISAWA J. The nucleolar protein Myb-binding protein 1A (MYBBP1A) enhances p53 tetramerization and acetylation in response to nucleolar disruption. J Biol Chem. 2014; 289:4928–40. [PubMed: 24375404]

RAVER-SHAPIRA N, MARCIANO E, MEIRI E, SPECTOR Y, ROSENFELD N, MOSKOVITS N, BENTWICH Z, OREN M. Transcriptional activation of miR-34a contributes to p53-mediated apoptosis. Mol Cell. 2007; 26:731–43. [PubMed: 17540598]

REDIS RS, VELA LE, LU W, FERREIRA DE OLIVEIRA J, IVAN C, RODRIGUEZ-AGUAYO C, ADAMOSKI D, PASCULLI B, TAGUCHI A, CHEN Y, FERNANDEZ AF, VALLEDOR L, VAN ROOSBROECK K, CHANG S, SHAH M, KINNEBREW G, HAN L, ATLASI Y, CHEUNG LH, HUANG GY, MONROIG P, RAMIREZ MS, CATELA IVKOVIC T, VAN L, LING H, GAFA R, KAPITANOVIC S, LANZA G, BANKSON JA, HUANG P, LAI SY, BAST RC, ROSENBLUM MG, RADOVICH M, IVAN M, BARTHOLOMEUSZ G, LIANG H, FRAGA MF, WIDGER WR, HANASH S, BERINDAN-NEAGOE I, LOPEZ-BERESTEIN G, AMBROSIO AL, GOMES DIAS SM, CALIN GA. Allele-Specific Reprogramming of Cancer Metabolism by the Long Non-coding RNA CCAT2. Mol Cell. 2016; 61:520–34. [PubMed: 26853146]

RILEY T, SONTAG E, CHEN P, LEVINE A. Transcriptional control of human p53-regulated genes. Nat Rev Mol Cell Biol. 2008; 9:402–12. [PubMed: 18431400]

RINN JL, KERTESZ M, WANG JK, SQUAZZO SL, XU X, BRUGMANN SA, GOODNOUGH LH, HELMS JA, FARNHAM PJ, SEGAL E, CHANG HY. Functional demarcation of active and silent chromatin domains in human HOX loci by noncoding RNAs. Cell. 2007; 129:1311–23. [PubMed: 17604720]

SANCHEZ Y, SEGURA V, MARIN-BEJAR O, ATHIE A, MARCHESE FP, GONZALEZ J, BUJANDA L, GUO S, MATHEU A, HUARTE M. Genome-wide analysis of the human p53 transcriptional network unveils a lncRNA tumour suppressor signature. Nat Commun. 2014; 5:5812. [PubMed: 25524025]

SCHLACKOW M, NOJIMA T, GOMES T, DHIR A, CARMO-FONSECA M, PROUDFOOT NJ. Distinctive Patterns of Transcription and RNA Processing for Human lincRNAs. Mol Cell. 2017; 65:25–38. [PubMed: 28017589]

SCHMITT AM, GARCIA JT, HUNG T, FLYNN RA, SHEN Y, QU K, PAYUMO AY, PERES-DA-SILVA A, BROZ DK, BAUM R, GUO S, CHEN JK, ATTARDI LD, CHANG HY. An inducible long noncoding RNA amplifies DNA damage signaling. Nat Genet. 2016; 48:1370–1376. [PubMed: 27668660]

TANG HY, ZHAO K, PIZZOLATO JF, FONAREV M, LANGER JC, MANFREDI JJ. Constitutive expression of the cyclin-dependent kinase inhibitor p21 is transcriptionally regulated by the tumor suppressor protein p53. J Biol Chem. 1998; 273:29156–63. [PubMed: 9786925]

TANI H, MIZUTANI R, SALAM KA, TANO K, IJIRI K, WAKAMATSU A, ISOGAI T, SUZUKI Y, AKIMITSU N. Genome-wide determination of RNA stability reveals hundreds of short-lived noncoding transcripts in mammals. Genome Res. 2012; 22:947–56. [PubMed: 22369889]

TANI H, NAKAMURA Y, IJIRI K, AKIMITSU N. Stability of MALAT-1, a nuclear long non-coding RNA in mammalian cells, varies in various cancer cells. Drug Discov Ther. 2010; 4:235–9. [PubMed: 22491206]

TRIPATHI V, ELLIS JD, SHEN Z, SONG DY, PAN Q, WATT AT, FREIER SM, BENNETT CF, SHARMA A, BUBULYA PA, BLENCOWE BJ, PRASANTH SG, PRASANTH KV. The nuclear-retained noncoding RNA MALAT1 regulates alternative splicing by modulating SR splicing factor phosphorylation. Mol Cell. 2010; 39:925–38. [PubMed: 20797886]

TRIPATHI V, SHEN Z, CHAKRABORTY A, GIRI S, FREIER SM, WU X, ZHANG Y, GOROSPE M, PRASANTH SG, LAL A, PRASANTH KV. Long noncoding RNA MALAT1 controls cell cycle progression by regulating the expression of oncogenic transcription factor B-MYB. PLoS Genet. 2013; 9:e1003368. [PubMed: 23555285]

TSOI LC, IYER MK, STUART PE, SWINDELL WR, GUDJONSSON JE, TEJASVI T, SARKAR MK, LI B, DING J, VOORHEES JJ, KANG HM, NAIR RP, CHINNAIYAN AM, ABECASIS GR, ELDER JT. Analysis of long non-coding RNAs highlights tissue-specific expression patterns and epigenetic profiles in normal and psoriatic skin. Genome Biol. 2015; 16:24. [PubMed: 25723451]

ULITSKY I, BARTEL DP. lincRNAs: Genomics, Evolution, and Mechanisms. Cell. 2013; 154:26–46. [PubMed: 23827673]

VILLUNGER A, MICHALAK EM, COULTAS L, MULLAUER F, BOCK G, AUSSERLECHNER MJ, ADAMS JM, STRASSER A. p53- and drug-induced apoptotic responses mediated by BH3-only proteins puma and noxa. Science. 2003; 302:1036–8. [PubMed: 14500851]

VOGELSTEIN B, LANE D, LEVINE AJ. Surfing the p53 network. Nature. 2000; 408:307–10. [PubMed: 11099028]

VOUSDEN KH, LANE DP. p53 in health and disease. Nat Rev Mol Cell Biol. 2007; 8:275–83. [PubMed: 17380161]

YOUNGER ST, KENZELMANN-BROZ D, JUNG H, ATTARDI LD, RINN JL. Integrative genomic analysis reveals widespread enhancer regulation by p53 in response to DNA damage. Nucleic Acids Res. 2015; 43:4447–62. [PubMed: 25883152]

Highlights

- PURPL is a p53-regulated lncRNA
- p53 is upregulated upon loss of PURPL, inducing growth defects
- PURPL associates with the p53-regulator, MYBBP1A
- PURPL suppresses p53 levels by inhibiting the p53-MYBBP1A interaction

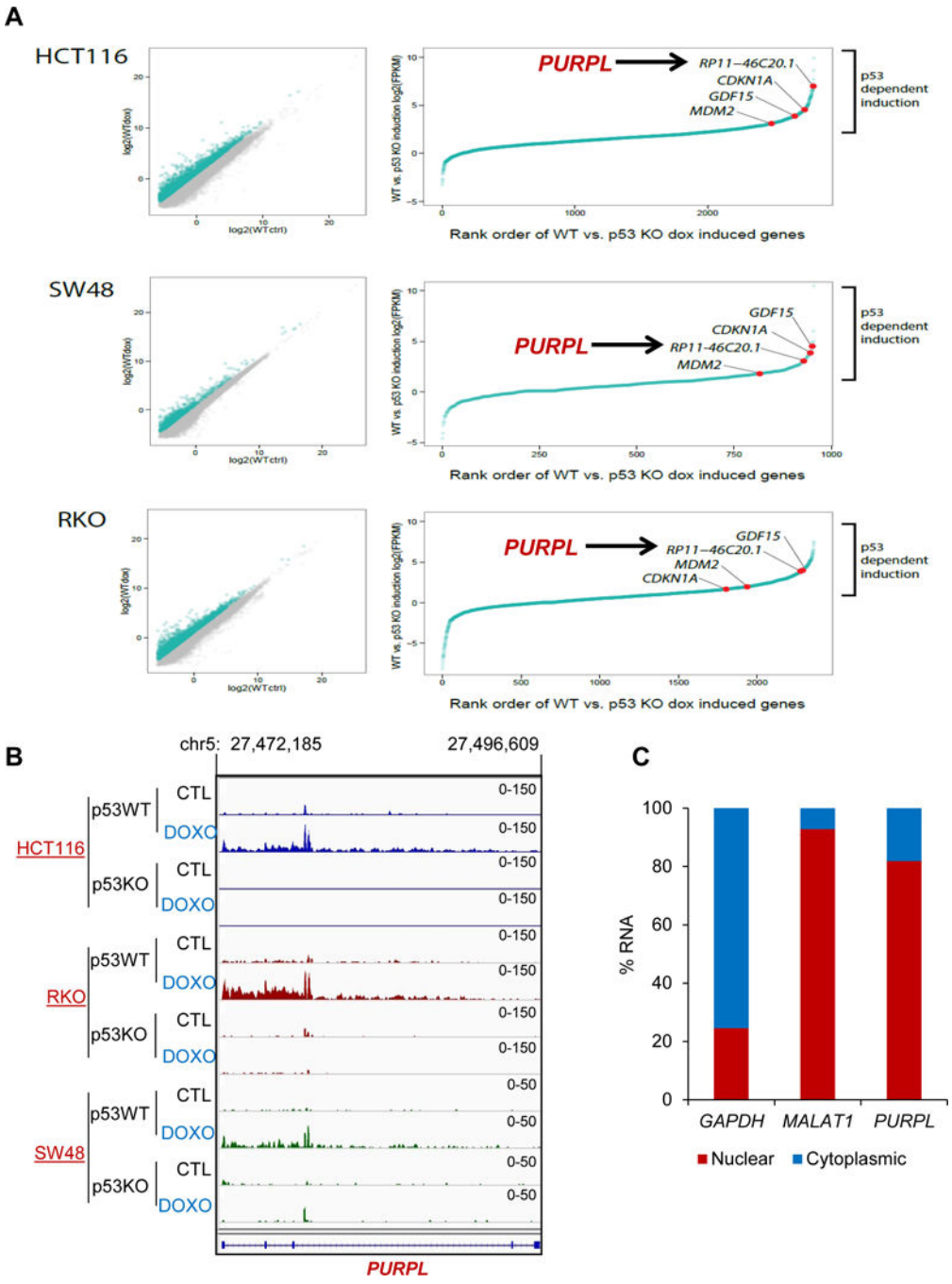

Figure 1. RNA-seq from multiple CRC lines identifies *PURPL* as a p53-regulated lncRNA

RNA-seq was performed from isogenic (p53WT and p53KO) HCT116, RKO and SW48 cells. **(A)** Scatter plot (left), Rank order of gene expression (right) and RNA-seq snapshot. **(B)** p53-dependent induction of *PURPL* (*RP11-46C20.1*) after DOXO treatment. **(C)** RT-qPCR for *PURPL* from nuclear and cytoplasmic fractions of untreated HCT116 cells. The cytoplasmic *GAPDH* mRNA and nuclear lncRNA *MALAT1* were used as controls.

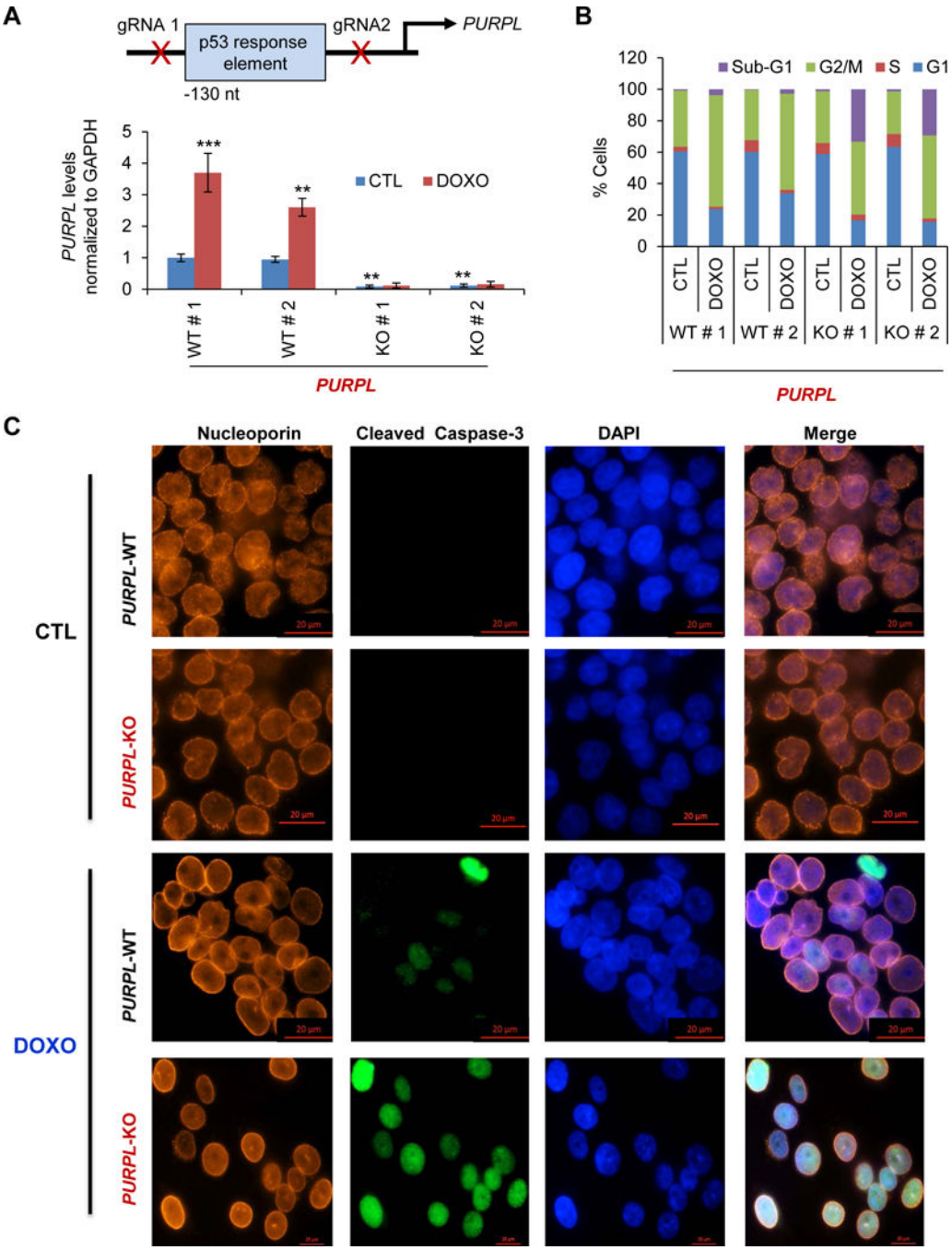

Figure 2. Targeted disruption of the p53RE in *PURPL* uncovers a pro-survival function of *PURPL*

(A) (Top) Schematic showing the p53RE in the *PURPL* promoter and location of the guide RNAs. (Bottom) RT-qPCR analysis from HCT116 *PURPL*-WT cells (WT#1 and WT#2) and HCT116 *PURPL*-KO cells (KO#1 and KO#2) untreated or treated with DOXO for 16 hr. **(B)** *PURPL*-WT and *PURPL*-KO cells were untreated or treated with DOXO for 48 hr; cell death (sub-G1 cells) and effect on cell cycle was assessed by PI staining followed by FACS analysis. **(C)** Immunostaining for Nucleoporin and cleaved caspase-3 from *PURPL*-WT and

PURPL-KO clones with or without DOXO treatment (72 hr). DNA was counterstained with DAPI. Error bars represent SD from 3 experiments. **p<0.01 and ***p<0.001.

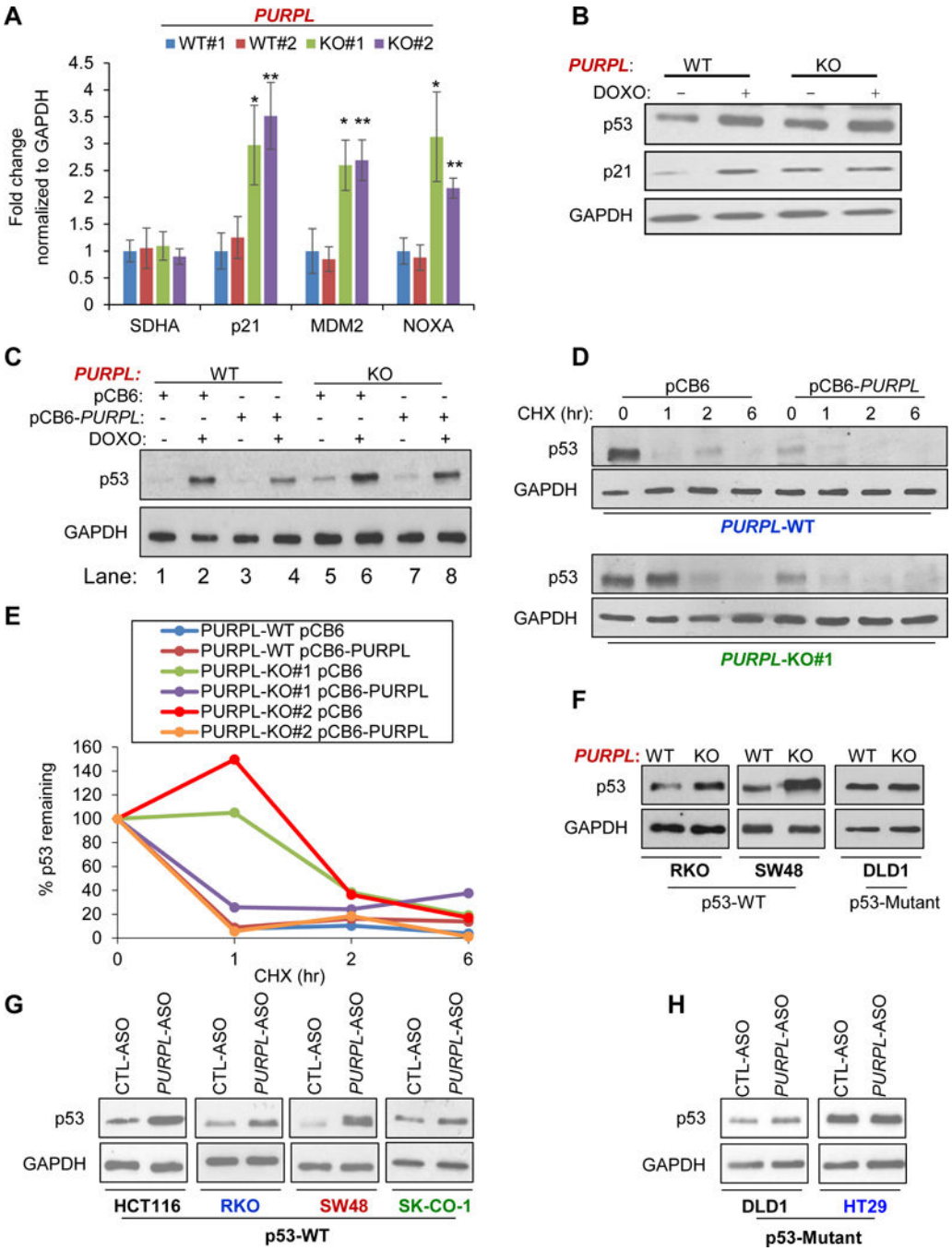

Figure 3. Loss of *PURPL* results in upregulation of basal p53 levels

(A) RT-qPCR analysis for select p53-regulated mRNAs and the housekeeping mRNA *SDHA* from untreated *PURPL*-WT and *PURPL*-KO cells. **(B)** *PURPL*-WT and *PURPL*-KO cells were untreated or treated with DOXO for 24 hr and immunoblotting for p53, p21 and the loading control GAPDH was performed. (**C**) Immunoblotting was performed from *PURPL*-WT and *PURPL*-KO#1 cells transfected for 48 hr with pCB6 or pCB6-*PURPL* followed by DOXO for 16 hr. GAPDH was used as loading control. **(D)** *PURPL*-WT and *PURPL*-KO#1 cells were transfected for 48 hr with pCB6 or pCB6-*PURPL* and then treated with

Cycloheximide (CHX) for the indicated times; immunoblotting for p53 and the loading control GAPDH was performed. **(E)** Decay curve for p53 protein quantitated by densitometry is shown for the immunoblot shown in Figures 3D and S9. **(F)** Immunoblotting for p53 and the loading control GAPDH was performed from *PURPL*-WT and *PURPL*-KO RKO, SW48 and DLD1 cells. **(G, H)** Parental HCT116, RKO, SW48, SK-CO-1, DLD1 and HT29 were transfected for 48 hr with CTL-ASO or *PURPL*-ASO and the levels of p53 and the loading control GAPDH were assessed by immunoblotting. Error bars represent SD from 3 experiments. *$p<0.05$ and **$p<0.01$.

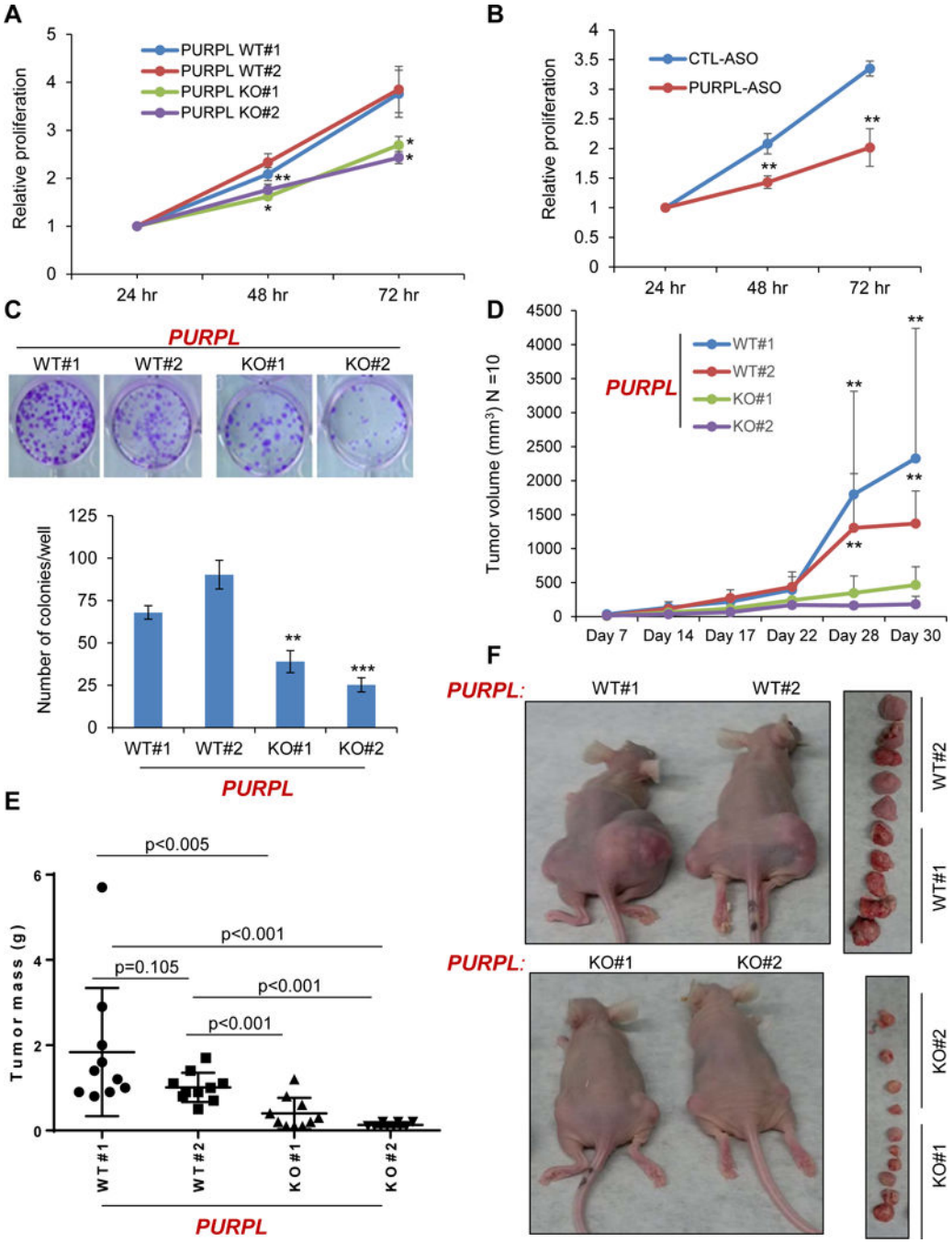

Figure 4. ***PURPL*-deficient cells show reduced proliferation *in vitro* and impaired tumor growth *in vivo***

(A) Cell proliferation assays determined by Cell counting Kit-8 at the indicated time points were performed from untreated *PURPL*-WT and *PURPL*-KO cells 24 hr after seeding the cells in 96-well plates. **(B)** HCT116 cells were transfected with a CTL-ASO or *PURPL*-ASO (50 nM) and cell proliferation assays were performed as described in "(A)". **(C)** Untreated *PURPL*-WT and *PURPL*-KO cells were seeded at low density in 12-well plates and colony formation assays were performed after 2 weeks. **(D)** Tumor volume (N=10 mice/

each group) in mice was measured by caliper assessment after injecting *PURPL*-WT and *PURPL*-KO cells in mice. **(E, F)** Mice were euthanized after 30 days, tumors were excised and weighed. Average tumor mass at Day 30 is shown (E). Error bars represent SD from 3 experiments in A–C. *p<0.05, **p<0.01 and ***p<0.001.

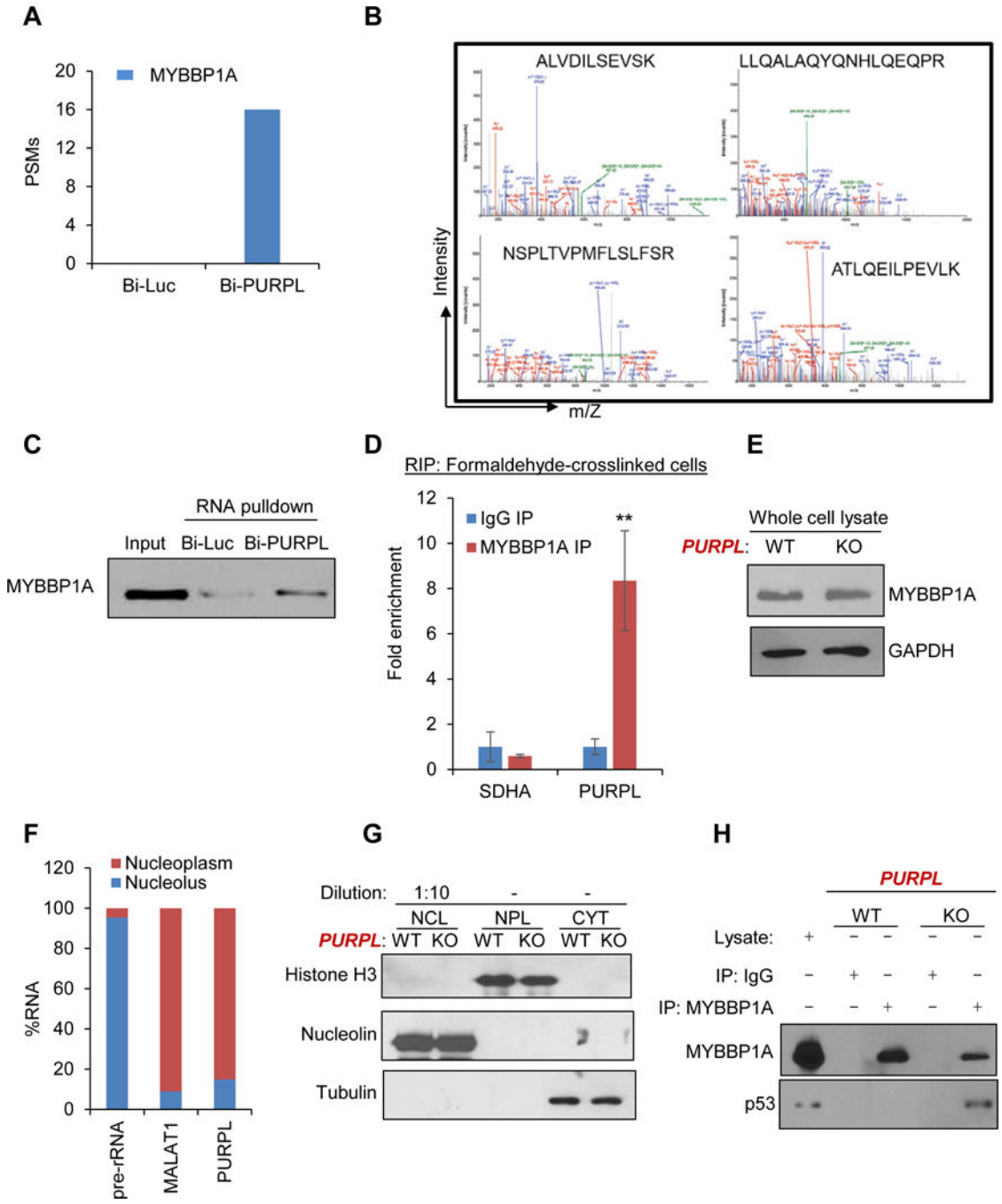

Figure 5. *PURPL* associates with MYBBP1A and prevents the formation of a p53-MYBBP1A complex

(A, B) RNA pulldowns were performed using *in vitro*-transcribed biotinylated *PURPL* (Bi-*PURPL*) RNA or biotinylated luciferase (Bi-*Luc*) RNA and HCT116 whole cell lysates. Associated proteins were pulled down with streptavidin beads and analyzed by SDS-PAGE and mass spectrometry. **(A)** Peptide spectrum matches (PSMs) corresponding to MYBBP1A in the Bi-*Luc* and Bi-*PURPL* pulldowns from mass spectrometry analysis, and **(B)** spectra, show the four MYBBP1A peptides that associate with *PURPL* in the RNA pulldowns and

mass spectrometry. **(C)** RNA pulldowns were performed as described in ‘A” followed by immunoblotting for MYBBP1A. **(D)** The enrichment of *PURPL* was measured by RT-qPCR from MYBBP1A RNA IPs (RIP) performed from formaldehyde-crosslinked HCT116 cells. IgG IP and the housekeeping *SDHA* mRNA were used as negative controls. **(E)** Immunoblotting for MYBBP1A and the loading control GAPDH was performed from *PURPL*-WT and *PURPL*-KO HCT116 whole cell lysates. **(F)** Nucleoplasmic and nucleolar fractions were prepared from HCT116 cells and the levels of the nucleolar pre-rRNA, the nucleoplasmic *MALAT1* and *PURPL* were measured by RT-qPCR. **(G)** Nucleoplasmic (NPL), nucleolar (NCL) and cytoplasmic (CYT) fractions were prepared from *PURPL*-WT and *PURPL*-KO cells and the levels of Histone H3, Nucleolin and Tubulin were assessed as controls for Nucleoplasmic, nucleolar and cytoplasmic fractions, respectively. **(H)** The interaction of MYBBP1A with p53 was determined by immunoblotting following co-IPs from *PURPL*-WT and *PURPL*-KO nucleoplasmic extracts. Lysate refers to whole cell extract prepared from *PURPL*-WT cells. Error bars represent SD from 3 experiments. **p<0.01.

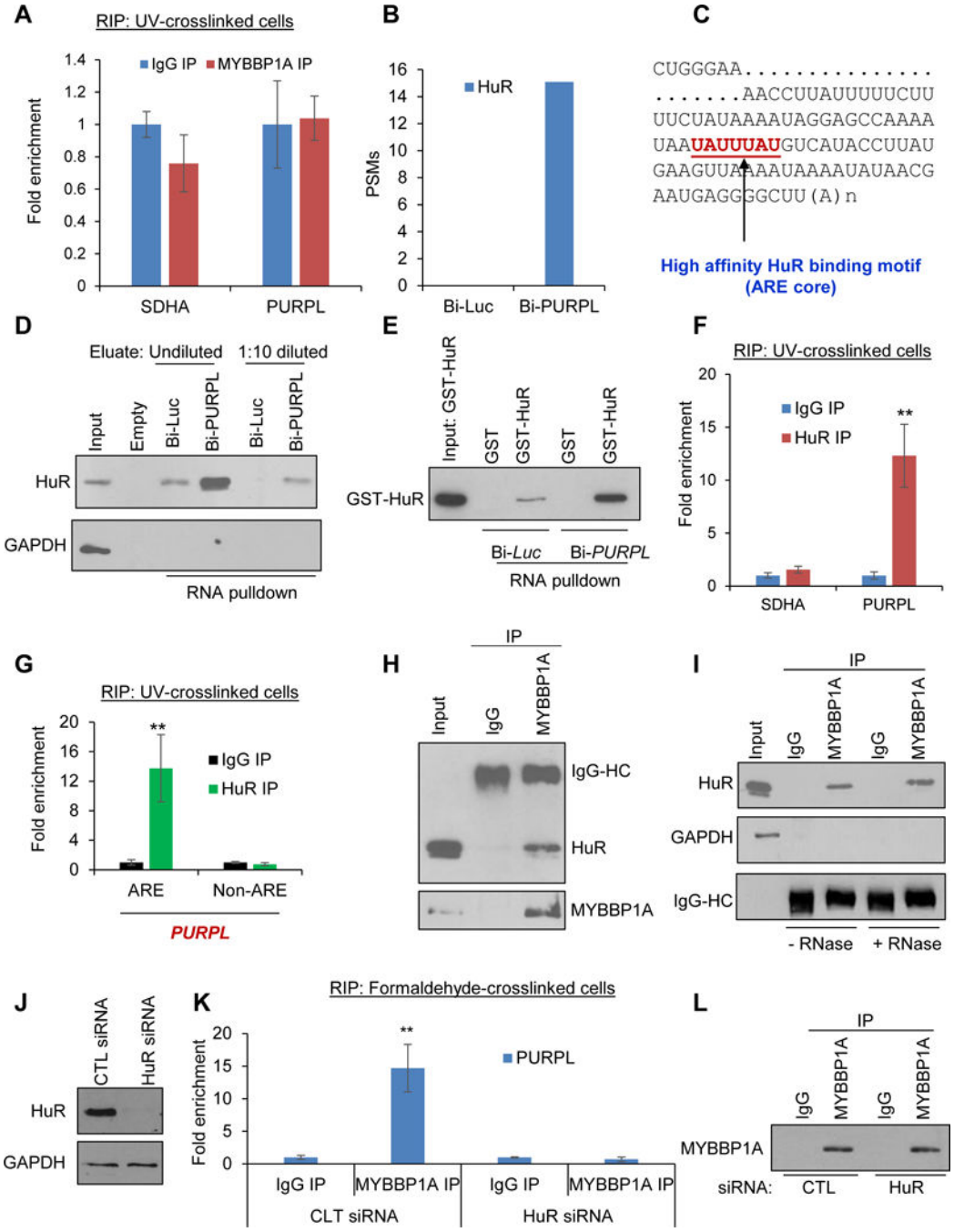

Figure 6. *PURPL* associates with MYBBP1A via the adaptor protein HuR

(A) *In vivo* UV-crosslinked HCT116 cells were subjected to RNA immunoprecipitation (RIP) with anti-MYBBP1A or IgG antibody. The levels of *PURPL* or the housekeeping *SDHA* mRNA were measured in the IP material by RT-qPCR. **(B)** Peptide spectrum matches (PSMs) corresponding to HuR in the Bi-*Luc* and Bi-*PURPL* pulldowns from mass spectrometry analysis is shown. **(C)** Partial sequence of *PURPL* RNA and the consensus high affinity HuR binding motif (UAUUUAU) at the 3′end is shown. **(D)** Streptavidin pulldowns were performed using HCT116 whole cell lysates and *in vitro* transcribed Bi-*Luc*

or Bi-*PURPL* and the eluted material (undiluted or 1:10 diluted) was subjected to immunoblotting for HuR or the negative control GAPDH. **(E)** Bi-*Luc* or Bi-*PURPL* were incubated with GST or GST-HuR and the mixture was then added to streptavidin beads. Enrichment of GST-HuR in the RNA pulldowns was determined by immunoblotting for HuR. **(F)** RNA IPs (RIP) assays were performed from UV-crosslinked HCT116 cell lysates using HuR antibody or IgG. Enrichment of *PURPL* in the IP material was assessed by RT-qPCR. *SDHA* mRNA was used as negative control. **(G)** RIP assays using HuR antibody or IgG were performed after sonicating UV-crosslinked HCT116 cell lysates. Enrichment of *PURPL*-ARE and not the nearby Non-ARE sequence in *PURPL* in the IP material was assessed by RT-qPCR normalized to *GAPDH* using primers that span the ARE or Non-ARE region. **(H)** HuR-MYBBP1A interaction was examined in HCT116 cells by immunoprecipitating MYBBP1A from whole cell lysates followed by immunoblotting for HuR and MYBBP1A. IgG IP was used as control. “IgG-HC” refers to the IgG heavy chain. **(I)** MYBBP1A was immunoprecipitated from HCT116 whole cell lysates and the enrichment of HuR in the IP material was assessed by immunoblotting in the presence or absence of RNase A. GAPDH was used as negative control. IgG-HC refers to the IgG heavy chain. **(J)** HCT116 cells were transfected with CTL siRNA or *HuR* siRNAs for 48 hr and knockdown of HuR was determined by immunoblotting using GAPDH as loading control. **(K)** RIP assays were performed from formaldehyde-crosslinked HCT116 cell lysates transfected with CTL siRNA or *HuR* siRNAs. Enrichment of *PURPL* normalized to *GAPDH* mRNA in the IP material was assessed by RT-qPCR. **(L)** Immunoblotting for MYBBP1A was performed for the RIP assays in “K”. Error bars represent SD from 3 experiments. **p<0.01.

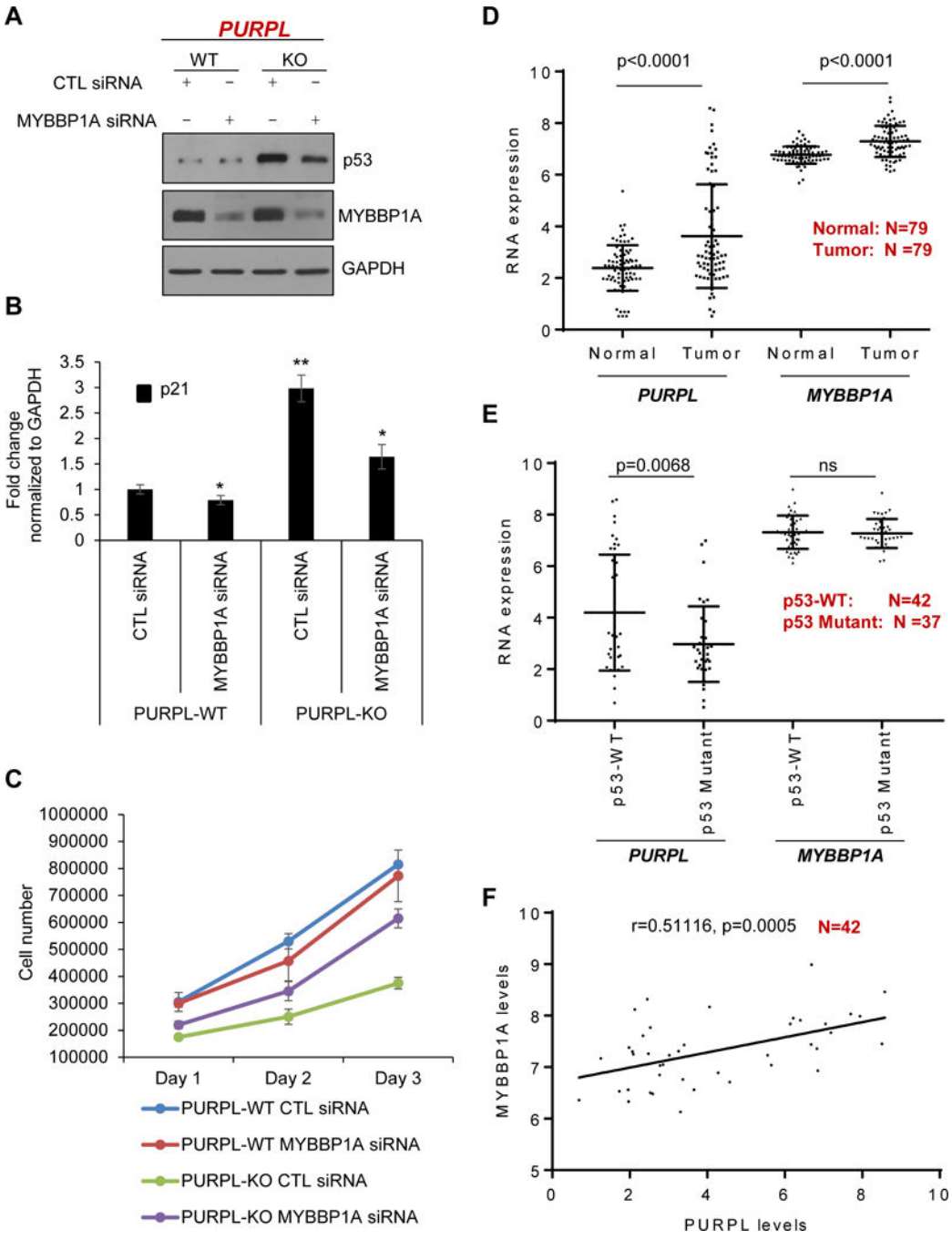

Figure 7. Silencing MYBBP1A in *PURPL*-KO cells partially rescues basal p53 levels and cell proliferation

(A, B) *PURPL*-WT and *PURPL*-KO cells were transfected with CTL siRNA or *MYBBP1A* siRNAs for 48 hr. The levels of MYBBP1A, p53 and the loading control GAPDH were assessed by immunoblotting from whole cell extracts (A) and *p21* mRNA levels were measured by RT-qPCR normalized to *GAPDH* mRNA (B). **(C)** *PURPL*-WT and *PURPL*-KO cells were transfected with CTL siRNA or *MYBBP1A* siRNAs and cell proliferation was assessed by trypan blue exclusion cell count assay from 2 independent experiments. **(D–**

F) Analysis of *PURPL* and *MYBBP1A* mRNA levels in CRC patient samples in the microarrays from the UMMC cohort. *PURPL* and *MYBBP1A* mRNA levels (log2 transformed) were compared between normal (N=79) and tumor (N=79) samples (D) and between p53WT (N=42) and mutant p53 tumors (N=37) (E). **(F)** Significant positive correlation (correlation coefficient shown as “r”) between *PURPL* and *MYBBP1A* mRNA levels was observed in the p53WT CRC tumors. “N” represents the number of samples in D–F. Error bars in “B” represent SD from 3 experiments. *p<0.05 and **p<0.01.